Criticality in single-distance phase retrieval

Ralf Hofmann,[1] **Julian Moosmann,**[2,*] **and Tilo Baumbach**[1,2]

[1]*Institut für Synchrotronstrahlung (ISS), Karlsruher Institut für Technologie (KIT), Hermann-von-Helmholtz-Platz 1, D-76344 Eggenstein-Leopoldshafen, Germany*
[2]*Laboratorium für Applikationen der Synchrotronstrahlung (LAS), Karlsruher Institut für Technologie (KIT), Postfach 6980, D-76128 Karlsruhe, Germany*

**julian.moosmann@kit.edu*

Abstract: We investigate why in free-space propagation single-distance phase retrieval based on a modified contrast-transfer function of linearized Fresnel theory yields good results for moderately strong pure-phase objects. Upscaling phase-variations in the exit plane, the growth of maxima of the modulus of the Fourier transformed intensity contrast dominates the minima. Cutting out small regions around the latter thus keeps information loss due to nonlocal, nonlinear effects negligible. This quasiparticle approach breaks down at a critical upscaling where the positions of the minima start to move rapidly. We apply our results to X-ray data of an early-stage Xenopus (frog) embryo.

© 2011 Optical Society of America

OCIS codes: (340.7440) X-ray imaging; (100.3010) Image reconstruction techniques; (100.5070) Phase retrieval; (100.2960) Image analysis.

References and links

1. A. Snigirev, I. Snigireva, V. Kohn, S. Kuznetsov, and I. Schelokov, "On the possibilities of Xray phase contrast microimaging by coherent high-energy synchrotron radiation," Rev. Sci. Instrum. **66**, 5486–5492 (1995).
2. S. W. Wilkins, T. E. Gureyev, D. Gao, A. Pogany, and A. W. Stevenson, "Phase-contrast imaging using polychromatic hard X-rays," Nature **384**, 335–338 (1996).
3. K. A. Nugent, T. E. Gureyev, D. F. Cookson, D. M. Paganin, and Z. Barnea, "Quantitative phase imaging using hard X rays," Phys. Rev. Lett. **77**, 2961–2964 (1996).
4. P. Cloetens, "Contribution to phase contrast imaging, reconstruction and tomography with hard synchrotron radiation," PhD dissertation, Vrije Universiteit Brussel (1999).
5. P. Cloetens, W. Ludwig, J. Baruchel, J.-P. Guigay, P. Rejmankova-Pernot, M. Salome, M. Schlenker, J. Y. Buffiere, E. Maire, and G. Peix, "Hard X-ray phase imaging using simple propagation of a coherent synchrotron radiation beam," J. Phys. D: Appl. Phys. **32**, A145–A151 (1999).
6. S. Zabler, P. Cloetens, J.-P. Guigay, J. Baruchel, and M. Schlenker, "Optimization of phase contrast imaging using hard X rays," Rev. Sci. Instrum. **76**, 073705 (2005).
7. M. R. Teague, "Deterministic phase retrieval: a Greens function solution," J. Opt. Soc. Am. **73**, 1434–1441 (1983).
8. J.-P. Guigay, "Fourier transform analysis of Fresnel diffraction patterns and in-line holograms," Optik **49**, 121–125 (1977).
9. T. E. Gureyev, Y. Nesterets, D. Paganin, A. Pogany, and S. Wilkins, "Linear algorithms for phase retrieval in the Fresnel region. 2. partially coherent illumination," Opt. Commun **259**, 569–580 (2006).
10. J. Moosmann, R. Hofmann, and T. Baumbach, "Single-distance phase retrieval at large phase shifts," Opt. Express **19**, 12066–12073 (2011).
11. L. D. Landau, "The theory of a Fermi liquid," Sov. Phys. JETP **3**, 920–925 (1957).
12. J. Goldstone, "Field theories with superconductor solutions," Nuovo Cimento **19**, 154–164 (1961).
13. J. Goldstone, A. Salam, and S. Weinberg, "Broken symmetries," Phys. Rev. **127**, 965–970 (1962).
14. Y. Nambu, "Quasiparticles and gauge invariance in the theory of superconductivity," Phys. Rev. **117**, 648–663 (1960).

#154861 - $15.00 USD Received 16 Sep 2011; revised 21 Oct 2011; accepted 26 Oct 2011; published 5 Dec 2011

15. F. Zernike, "Phase-contrast, a new method for microscopic observation of transparent objects. Part I.," Physica **9**, 686–698 (1942).
16. F. Zernike, "Phase-contrast, a new method for microscopic observation of transparent objects. Part II.," Physica **9**, 974–986 (1942).
17. J. Moosmann, V. Altapova, D. Hänschke, R. Hofmann, and T. Baumbach, "Nonlinear, noniterative, single-distance phase retrieval and developmental biology," submitted to AIP Proceedings, ICXOM 21.

With the advent of 3rd-generation synchrotron light sources, producing highly intense and spatially coherent X-rays, the investigation of materials of low absorption but considerable phase-shifting capability can be and is routinely performed. This opens up the potential for the application of new, nondestructive imaging techniques relevant to in vivo investigation of biological samples. Moreover, satisfactory phase retrieval from a single-distance projection in free-space propagation in combination with the small exposure times due to large photon fluxes at synchrotron beamlines enable time resolved tomographic imaging for the study of evolution processes on the cellular and subcellular level. Therefore, in particular the field of developmental biology should benefit from the method discussed in this paper.

For monochromatic and parallel X-ray illumination (wave number $k = \frac{2\pi}{\lambda} = \frac{2\pi E}{hc}$, wave length λ, circular frequency ω, energy E, quantum of action h, speed of light in vacuum c) of a pure-phase object, which does not diminish the (ideal) spatial coherence properties of the incoming wavefront, we consider free-space propagation of the modulated exit wavefront $\psi_{z=0}(\vec{r})$ away from plane $z=0$ to generate intensity contrast $g_z \equiv \frac{I_z - I_{z=0}}{I_{z=0}}$ at distance $z > 0$ [1–7]. Here I_z is the intensity measured in plane z, and $I_{z=0} \equiv \text{const}$ for a pure-phase object. In such a setting, we consider phase retrieval based on a projected version of the *contrast-transfer function* (CTF) [8], which represents a *linear* and *local* [9] relation between g_z and the phase shift $\phi_{z=0}$ exiting the object, when $\phi_{z=0}$ violates the CTF criterion

$$\left| \phi_{z=0}\left(\vec{r} - \frac{\pi z}{k}\vec{\xi}\right) - \phi_{z=0}\left(\vec{r} + \frac{\pi z}{k}\vec{\xi}\right) \right| \ll 1\,. \tag{1}$$

Here $\vec{\xi}$ is a transverse-plane wave vector. Such a regularized form of CTF retrieval, named *projected CTF*, was proposed in [10] and yields, via the local retrieval of an *effective* phase in the spirit of a quasiparticle model [11], remarkably good results for single-distance phase retrieval. The present paper aims at a deeper understanding of this situation.

In Fresnel theory the following important relation holds [8]

$$(\mathscr{F} I_z)(\vec{\xi}) = \int d^2r \, \exp(-2\pi i \vec{r}\cdot\vec{\xi}) \times \psi_{z=0}\left(\vec{r} - \frac{\pi z}{k}\vec{\xi}\right) \psi^*_{z=0}\left(\vec{r} + \frac{\pi z}{k}\vec{\xi}\right), \tag{2}$$

where $\mathscr{F}$ denotes Fourier transformation in the transverse plane. Writing $\psi_{z=0} = \sqrt{I_{z=0}}\,\mathrm{e}^{i\phi_{z=0}}$ and expanding the exponential up to quadratic order in $\phi_{z=0}$ yields upon substitution into Eq. (2) and use of the Fourier convolution theorem

$$\begin{aligned}(\mathscr{F} g_z)(\vec{\xi}) &= 2\sin(s)\,(\mathscr{F}\phi_{z=0})(\vec{\xi}) - \cos(s)\int d^2\xi'\,(\mathscr{F}\phi_{z=0})(\vec{\xi}')(\mathscr{F}\phi_{z=0})(\vec{\xi}-\vec{\xi}') \\ &\quad + \mathrm{e}^{is}\int d^2\xi'\,\mathrm{e}^{-\frac{4\pi^2 iz\vec{\xi}\cdot\vec{\xi}'}{k}}(\mathscr{F}\phi_{z=0})(\vec{\xi}')(\mathscr{F}\phi_{z=0})(\vec{\xi}-\vec{\xi}') + O((\mathscr{F}\phi_{z=0})^3)\,,\end{aligned} \tag{3}$$

where $s \equiv \frac{2\pi^2 z\vec{\xi}^2}{k}$. CTF retrieval corresponds to a truncation of the right-hand side of Eq. (3) at *linear* order in $\mathscr{F}\phi_{z=0}$. Provided that $(\mathscr{F} g_z)(\vec{\xi})$ exhibits zeros of the same order as those of the sine function at $|\vec{\xi}|_n \equiv \sqrt{(kn)/(2\pi z)}$ $(n = 0,1,2,\cdots)$ CTF retrieval in Fourier space does not produce singularities. In analogy to quantum statistical mechanics, CTF represents a dispersion law between complex "energy" $(\mathscr{F}\, g_z)(\vec{\xi})$ and complex "momentum" $(\mathscr{F}\, \phi_{z=0})(\vec{\xi})$, both parameterized by $\vec{\xi}$. Being a linear model, the spectrum exhibits scaling symmetry: The ratio $\frac{\mathscr{F}\, g_z}{\mathscr{F}\, \phi_{z=0}}(\vec{\xi})$ is invariant under $\mathscr{F}\, g_z, \mathscr{F}\, \phi_{z=0} \to S\mathscr{F}\, g_z, S\mathscr{F}\, \phi_{z=0}$ where S is positive and real. The phase $\phi_{z=0}$ in position space and thus inverse Fourier transformation is understood as an average related to a "partition function" $Z_{\vec{r}}$: An $\vec{r}$ dependent "Hamiltonian" $\mathscr{H}_{\vec{r}} \equiv 2\pi\vec{\xi}\cdot\vec{r}$ is used to define $Z_{\vec{r}} \equiv \mathrm{tr}\exp(i\mathscr{H}_{\vec{r}})$ where the trace symbol is understood as a sum over all wave-vector states. Notice that changing the value of $\phi_{z=0} = \mathrm{tr}\left[(\mathscr{F}\, \phi_{z=0})\exp(i\mathscr{H}_{\vec{r}})\right]$ by a change of the measure-zero set $V_n \equiv \{(\mathscr{F}\, \phi_{z=0})(|\vec{\xi}|_n(\cos\theta, \sin\theta))|0 \le \theta \le 2\pi\}$, which is undetermined in CTF retrieval, possesses vanishing probability.

Scaling symmetry of the spectrum is exact in the trivial limit $\phi_{z=0} \to \alpha \equiv \mathrm{const}$. According to Eq. (2), then $(\mathscr{F}\, I_z)(\vec{\xi}) \equiv \delta^{(2)}(\vec{\xi})I_{z=0}$, thus $(\mathscr{F}\, g_z)(\vec{\xi}) \equiv 0$, and the right-hand side of Eq. (3) is $\frac{\delta^{(1)}(\vec{\xi}^2)}{2\pi}\sin(2\pi^2 z\vec{\xi}^2/k)\left(\alpha + i\alpha^2 + O(\alpha^3)\right)$. That is, the only state that occurs is the "vacuum" (state of zero "energy") at $\vec{\xi} = 0$. (The impossibility of retrieving α from this relation is due to a global U(1) or constant-phase-shift symmetry of Fresnel theory.) When $\phi_{z=0}$ starts to vary, infinitely many CTF "vacua" appear at $|\vec{\xi}|_n$, and excitations of finite "energy" occur in between these "vacua". Explicit violations of scaling symmetry are introduced by the nonlinear and nonlocal terms in Eq. (3) starting at $O((\mathscr{F}\, \phi_{z=0})^2)$. These cause CTF "vacua" to become "finite-energy" minima of $|\mathscr{F}\, g_z|$.

Let us now exemplarily investigate the effect in Eq. (3) of the quadratic, nonlocal correction to the CTF "dispersion law". To do so, we appeal to a 2D isotropic Gaussian model (GM) of the exit phase map, $\phi^{\mathrm{GM}}_{z=0}(\vec{r}) = \mathrm{e}^{-\frac{\vec{r}^2}{2\sigma^2}}$, where σ denotes the Gaussian's width, and the maximal, relative phase variation is unity. It is straight-forward to derive an expression for the right-hand side of Eq. (3) when evaluated in this model after letting $\phi^{\mathrm{GM}}_{z=0} \to S\,\phi^{\mathrm{GM}}_{z=0}$ (or $\mathscr{F}\, \phi^{\mathrm{GM}}_{z=0} \to S\,\mathscr{F}\, \phi^{\mathrm{GM}}_{z=0}$):

$$\begin{aligned}(\mathscr{F}\, g^{\mathrm{GM}}_z)(\vec{\xi}) &= \sigma^2\pi\Big[4\sin\left(\frac{2\pi^2 z}{k}\vec{\xi}^2\right)\mathrm{e}^{-2\pi^2\sigma^2\vec{\xi}^2}\, S \\ &\quad - \mathrm{e}^{-\pi^2\sigma^2\vec{\xi}^2}\left(\cos\left(\frac{2\pi^2 z}{k}\vec{\xi}^2\right) - \mathrm{e}^{-\pi^2\frac{z^2}{k^2\sigma^2}\vec{\xi}^2}\right)S^2\Big]\,.\end{aligned} \tag{4}$$

Let us compare the rates of change $\pi^2\sigma^2$ and $\pi^2\frac{z^2}{k^2\sigma^2}$ in the two exponentials appearing at order S^2. Their ratio is $\frac{\sigma^4 k^2}{z^2}$. For $\lambda = 10^{-10}\,\mathrm{m}$, $\sigma = 10^{-6}\,\mathrm{m}$, $z = 1\,\mathrm{m}$ this yields a value of $\frac{\pi^2}{2500} \ll 1$. Thus the exponential in the round brackets can be neglected. On the other hand, the ratio of the rates of change of the argument of the sine (and cosine) and the exponential factor $\mathrm{e}^{-2\pi^2\sigma^2\vec{\xi}^2}$ is $\frac{z}{k\sigma^2}$. For the above-assumed parameter values this yields a value of $\frac{50}{\pi} \gg 1$. Thus the sine and cosine factors vary much faster than the exponential factors, and we can treat the latter as constants as far as the investigation of a phase shift φ of the sine function (order S) as induced by the cosine correction (order S^2) in the vicinity of $|\vec{\xi}|^2_1 = \vec{\xi}^2_1 = \frac{k}{2\pi z}$ is concerned. Using $a\sin x + b\cos x = \sqrt{a^2+b^2}\sin(x+\varphi)$, where $\varphi = \arcsin\frac{b}{\sqrt{a^2+b^2}}$, we have at $\vec{\xi}^2_1$ to linear order in S and with the above parameter values a phase shift φ of the sine function in Eq. (4) given as

$$\varphi \sim \frac{1}{4}S\,\frac{1}{\sqrt{\mathrm{e}^{-2\pi^2\sigma^2\vec{\xi}^2} + \frac{S^2}{16}}}\Bigg|_{\vec{\xi}^2 = \vec{\xi}^2_1 = \frac{k}{2\pi z}} \sim \frac{1}{4}S\,. \tag{5}$$

Thus, for sufficiently small values of S, the shift of the first zero of the sine function as introduced by the quadratic, nonlocal corrections in Eq. (3) is negligible for the Gaussian model

#154861 - \$15.00 USD Received 16 Sep 2011; revised 21 Oct 2011; accepted 26 Oct 2011; published 5 Dec 2011
(C) 2011 OSA

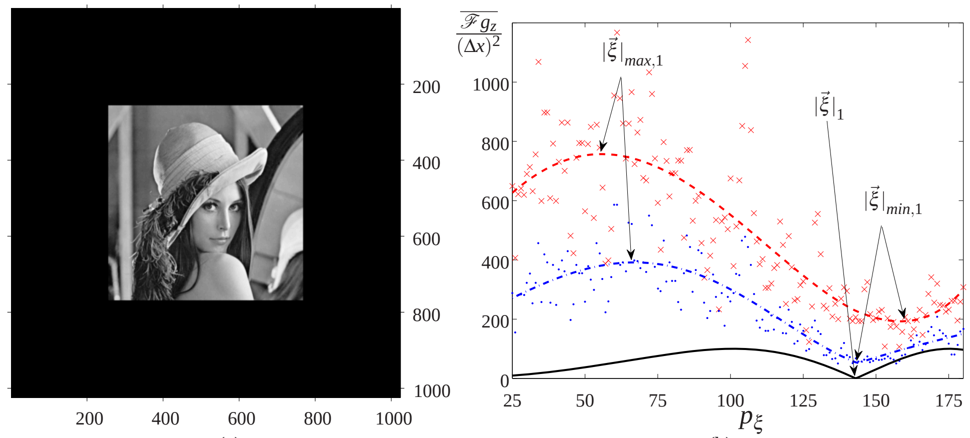

(a) (b)

Fig. 1. (a): transverse position-space phase map at $z = 0$ (zero padded test pattern Lena), (b): $\frac{\overline{\mathscr{F} g_z(|\vec{\xi}|)}}{(\Delta x)^2}$ at $E = 10\,\mathrm{keV}$, $z = 0.5\,\mathrm{m}$ and for $S = 200$ and $S = 450$, see text. The solid line is a plot of $100\,|\sin(2\pi^2 z|\vec{\xi}|^2/k)|$. Dots and crosses indicate the respective "data", dashed-dotted and dashed lines are respective fits to $F(t) \equiv c_1 \mathrm{e}^{-c_2 t^2 - c_3 t}|\sin(t^2)| + c_4 + c_5 t + c_6 t^2 + c_7 t^3 + c_8 t^4 + c_9 t^5$, where $t \equiv \pi\sqrt{\frac{2z\vec{\xi}^2}{k}}$, and $c_1, \cdots, c_9$ are real constants. The actual argument in the plots is the pixel number $p_\xi = L|\vec{\xi}|$ in Fourier space where $L = p_{x,max}\Delta x$, L^2 is area of the field of view, and $p_{x,max}$, Δx denote the maximal pixel number, resolution in transverse position space, respectively.

considered. We demonstrate below in a full numerical treatment of the Fresnel forward propagation for a generic, that is, realistically complex situation that the position of the first minima $|\vec{\xi}|_{min,1}$ does not move away from $|\vec{\xi}|_1 \equiv \sqrt{k/(2\pi z)}$ at all for a wide range of S values that upscale the regime where linear CTF retrieval is applicable. A critical increase of $|\vec{\xi}|_{min,1}$ sets in rather late at a maximal relative phase variation larger than unity. Therefore, the entirety of higher-order corrections to the right-hand side of Eq. (3) actually stabilizes our perturbative, Gaussian-model finding of a slow variation of $|\vec{\xi}|_1$ for small S to a situation of no variation at all up to S_c. Moreover, the all-order result changes a polynomial dependence of $|\vec{\xi}|_1$ on S, as it is obtained in finite-order perturbation theory, to a fractional power of $S - S_c$ for $0 < \frac{S-S_c}{S_c} \ll 1$.

The fact that the minima of the modulus of $\mathscr{F} g_z$ are not moving for $0 < S \leq S_c$ indicates that explicit scaling-symmetry violation is not supplemented by *dynamical* breaking all the way up to S_c. Recall that *explicit* symmetry breaking refers to the fact that finite as opposed to vanishing values of the "energy" $(\mathscr{F} g_z)(\vec{\xi})$ are no longer invariant under the symmetry. On the other hand, for the symmetry to be broken *dynamically* the locations, where minimal "energy" is attained, are shifted under the symmetry. For a continuous symmetry such as scaling symmetry the latter situation changes the spectrum drastically: It introduces new degrees of freedom (Goldstone bosons [12–14]), and the description in terms of the old spectrum is lost. In our case, this happens for $S \geq S_c$. (The quasiparticle concept leading to an effective CTF phase then is as useless as the description of an atomic crystal in terms of moderately interacting atoms which, however, applies to the liquid phase.) If condition (1) is sufficiently well satisfied then limited resolution in transverse Fourier space in any discretized formulation does not resolve the small-residue poles of CTF retrieval that appear in $\mathscr{F}\phi_{z=0}$ at $|\vec{\xi}|_n$, and numerical Fourier

#154861 - $15.00 USD Received 16 Sep 2011; revised 21 Oct 2011; accepted 26 Oct 2011; published 5 Dec 2011
(C) 2011 OSA

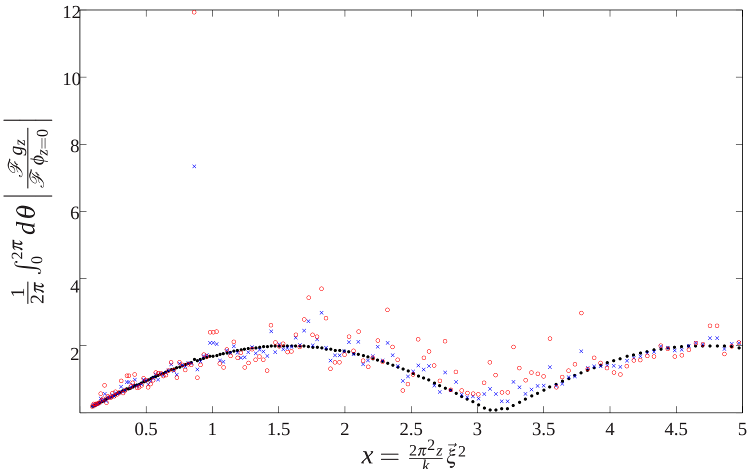

Fig. 2. Plot of the angular average of the modulus of the transfer function of the linear CTF approximation $\left|\frac{\mathscr{F} g_z}{\mathscr{F}\phi_{z=0}}\right|$ for various values of upscaling, $S = 1$ (solid black dots), $S = 100$ (blue crosses), and $S = 200$ (red circles), where $S = 1$ is associated with the phase map $\phi_{z=0,\mathrm{CTF}}$ (compare with Fig. 1(a)) at $\phi_{\max} = 0.01$.

inversion yields satisfactory phase retrieval. We define $\phi_{\max} \equiv \max\{\phi_{z=0}(\vec{r})\}$ with the convention that $0 \leq \phi_{z=0}(\vec{r})$. With our pixel resolution of $\Delta x = 1.1\,\mu$m, $E = 10$ keV, and $z = 0.5$ m we are in this CTF scaling regime when setting $\phi_{\max} = 0.01$ for the phase map $\phi_{z=0}$ in Fig. 1(a) which serves as an input to Fresnel forward propagation. In this case we refer to the phase map as $\phi_{z=0,\mathrm{CTF}}$. In Fig. 1(b) we show angular averages $\overline{\mathscr{F} g_z}(|\vec{\xi}|) \equiv \frac{1}{2\pi}\int_0^{2\pi} d\theta\, |\mathscr{F} g_z|(|\vec{\xi}|(\cos\theta, \sin\theta))$ (modulo a suitable treatment of truncation rods) as functions of $|\vec{\xi}|$ obtained for two inputs $\phi_{z=0} = S\phi_{z=0,\mathrm{CTF}}$ with $S = 200 < S_c = 356$ and $S = 450 > S_c$. ($S = 1$ corresponds to $\phi_{z=0,\mathrm{CTF}}$.) While for $S = 200$ the position of $|\vec{\xi}|_{\min,1}$ coincides with the CTF "vacuum" $|\vec{\xi}|_1$ this is not true for $S = 450$. "Finite-energy" minima at $S = 200$ introduce poles in Fourier space and thus quasiperiodic artifacts [10] into position-space CTF retrieval. To cope with this, the following projection is applied [10]

$$(\mathscr{F} g_z)(\vec{\xi}) \to \Theta\left(\left|\sin\left(\frac{2\pi^2 z}{k}\vec{\xi}^2\right)\right| - \varepsilon\right) \times (\mathscr{F} g_z)(\vec{\xi})\,, \tag{6}$$

where $\frac{2\pi^2 z}{k}\vec{\xi}^2 > \frac{\pi}{2}$, Θ denotes the Heaviside step function, and ε is a threshold ($0 < \varepsilon < 1$) such that minima are centrally cut about the CTF "vacua". Applying CTF retrieval to the projected intensity contrast on the right-hand side of replacement (6) yields good results even for very small values of ε.

To show how scaling symmetry is increasingly broken in an explicit way within the window $1 \leq S \leq S_c$, where no dynamical breaking occurs, we have investigated in Fig. 2 the behavior of the transfer function of the CTF approximation in dependence of S for the phase map of Fig. 1(a). Observing a smooth sinusoidal shape for $S = 1$ justifies the above-mentioned consideration of $\phi_{max} = 0.01$ as a representative of the linear scaling regime. Notice the increasingly dramatic and nervous deviations from this sinusoidal dependence for $S = 100$ and $S = 200$. Therefore, we conclude that even for maximal phase shifts well below $S_c \times 0.01 \sim 3.6$ (moderately strong maximal phase variation) the assumed linearity of CTF retrieval fails judging by the behavior of the associated transfer function.

Let us now spell out the reasons for why projected CTF retrieval is good within the window

#154861 - $15.00 USD Received 16 Sep 2011; revised 21 Oct 2011; accepted 26 Oct 2011; published 5 Dec 2011
(C) 2011 OSA

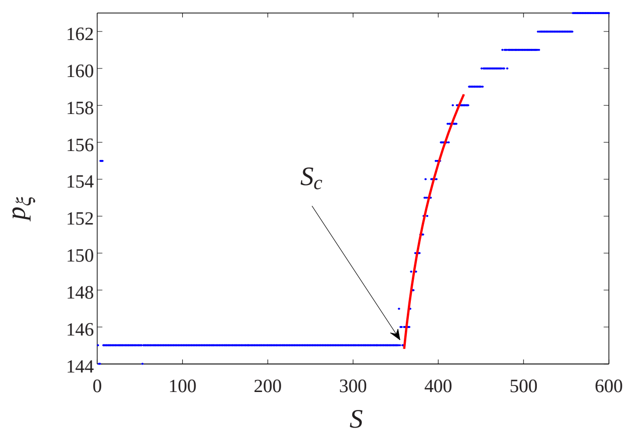

Fig. 3. Plot of pixel number p_ξ, which belongs to $|\vec{\xi}|_{min,1}$, as a function of S. Notice the onset of critical behavior (second-order like phase transition) to the right of $S_c = 356$. Notice also that the variance of $|\vec{\xi}|_{min,1}$ for $S < S_c$ practically is zero.

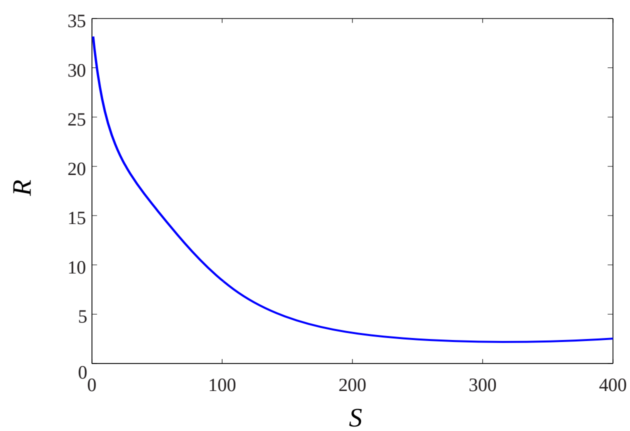

Fig. 4. Plot of function $R(S) \equiv \frac{v_{max,1}}{v_{min,1}}$. (The "data" $\overline{\mathscr{F}g_z}(|\vec{\xi}|_{max,1})(S)$ and $\overline{\mathscr{F}g_z}(|\vec{\xi}|_{min,1})(S)$ was fitted to 9th-degree polynomials, and the derivatives defining $v_{max,1}$ and $v_{min,1}$ were taken of these polynomials.)

$1 \le S \le S_c$. Figure 3 shows how the position of the first minimum $|\vec{\xi}|_{min,1}$ changes with increasing S. At $S_c = 356$, which corresponds to $\phi_{\max} \sim 3.6$ and thus to a profound violation of condition (1), a critical increase of $|\vec{\xi}|_{min,1}$ away from the first CTF "vacuum" $|\vec{\xi}|_1$ takes place. A fit to $A|S - S_c|^\nu + B$ (A, B, ν real, $S > S_c$) of this critical behavior, which resembles a second-order phase transition, yields an exponent $\nu \sim 0.15 \pm 0.1$, the large error being associated with instabilities w.r.t. the length of the fitting interval. ($|\vec{\xi}|_{min,1} - |\vec{\xi}|_1$ is only a pseudo-order parameter for dynamical scaling-symmetry breaking since the latter occurs on top of explicit breaking. For a discrete-symmetry analog, consider an Ising model with magnetic field H. For $H = 0$ the model is $\mathbf{Z_2}$ invariant, for $H \neq 0$ not. For $T \le T_c$ ferromagnetic ordering occurs, and, given moderate values of H, it makes sense to consider mean magnetization a pseudo-order parameter for *dynamical* $\mathbf{Z_2}$ breaking.)

Figure 4 depicts the ratio R of $v_{max,1} \equiv \frac{d\overline{\mathscr{F}g_z}(|\vec{\xi}|_{max,1})}{dS}$ and $v_{min,1} \equiv \frac{d\overline{\mathscr{F}g_z}(|\vec{\xi}|_{min,1})}{dS}$ as a function of S for $1 \le S \le S_c = 356$. Notice that for all such S the growth of the first maximum by far outraces that of the first minimum. This can be understood as follows. While, according to Eq. (3), the growth of the minima solely is due to the nonlocal terms at quadratic and higher order in $\mathscr{F}\,\phi_{z=0}$ there is a local component in the growth of the maxima (scaling proportional to S due to the linear and local CTF order in Eq. (3)). For reasonably "nervous" $\mathscr{F}\,\phi_{z=0}$ and for sufficiently moderate S successive n-fold autoconvolutions of $\mathscr{F}\,\phi_{z=0}$ ($n \geq 2$) tend to homogenize the nonlinear corrections, which are proportional to S^n, to small values. Thus, in this regime the dominantly linearly and locally driven growth of the maxima outraces the growth of the minima, and little information is lost if for $1 \leq S \leq S_c$ thin rings centered at $|\vec{\xi}|_n$ are cut out to enable singularity-free phase retrieval [10], see Eq. (6).

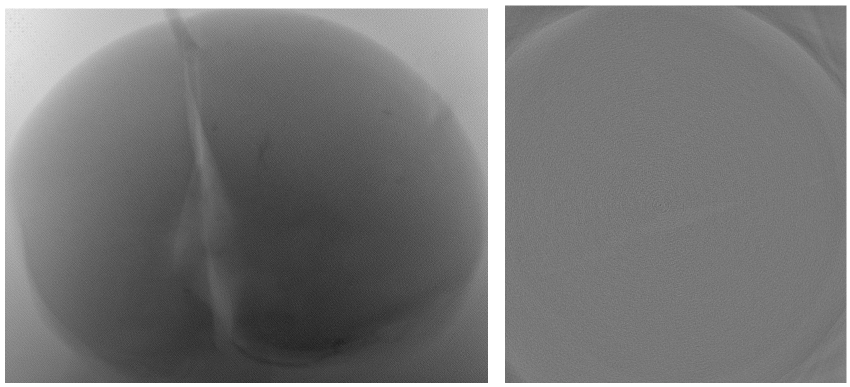

(a) (b)

Fig. 5. The CTF situation: (a) phase retrieval of a projection through the four-cell stage of a Xenopus embryo. The size of the projection is 1725 x 1338 pixel^2, or 1.3 x 1.0 mm^2. (b) 2-D slice of the tomographic reconstruction of the electron density. The data, compare with Fig. 6(a),(d), was taken at the ID19 beamline at ESRF with $E = 20\,\mathrm{keV}$ (monochromatized to $\frac{\Delta E}{E} = 10^{-4}$ using double Si 111 crystals), 1599 projections per tomogram, an exposure time per frame of 2 s, an effective pixel size of $0.745\,\mu\mathrm{m}$, and an object-detector distance of $z = 0.945\,\mathrm{m}$. The size of the slice is 1532 x 1691 pixel^2, or 1.14 x 1.25 mm^2. In both images large-scale variations were subtracted for better visibility.

Figures 5 and 6 show the results of an analysis of experimental data for phase contrast from the four-cell stage of a Xenopus embryo. Figure 5 indicates the uselessness of CTF retrieval in view of the considerable phase variations introduced by the object, and Fig. 6 points out the higher resolving power of projected CTF versus retrieval using the linearized transport-of-intensity equation (yolk particles clearly can be tracked in former case).

The following self-consistency test for projected CTF can be devised in applications to nearly pure-phase objects. Retrieve the phase $\phi^{\mathrm{pCTF}}_{z=0}(\vec{r})$ according to projected CTF (including a subtraction of large-scale variations arising from small absorption effects) from the measured intensity contrast $g_z(\vec{r})$, let $\phi^{\mathrm{pCTF}}_{z=0} \to S\,\phi^{\mathrm{pCTF}}_{z=0}$ with a moderate value of S, say, $S = 2$, Fresnel propagate $S\,\phi^{\mathrm{pCTF}}_{z=0}$ to z to generate the new intensity contrast $g^{\mathrm{S}}_z(\vec{r})$ and investigate whether, compared to $\overline{\mathscr{F}\,g_z}(|\vec{\xi}|) = \overline{\mathscr{F}\,g^{\mathrm{S=1}}_z}(|\vec{\xi}|)$, the minima $|\vec{\xi}|_{min,1}$ have moved in $\overline{\mathscr{F}\,g^{\mathrm{S}}_z}(|\vec{\xi}|)$. In Fig. 7 $\overline{\mathscr{F}\,g^{\mathrm{S}}_z}(|\vec{\xi}|)$ ($S = 1,2$) are depicted for projected CTF applied to the Xenopus data of Fig. 6(a),(d), and it is obvious that $|\vec{\xi}|_{\mathrm{min,1}}$ did not move. Thus we conclude that projected CTF retrieval self-consistently operates within its regime of validity for this particular experiment.

To summarize, we have in a quite generic way shown why the local (quasiparticle) approach to single-distance phase retrieval yields robust and good results. Specifically, we have considered the behavior of the angular averaged modulus of the Fourier transform of the intensity

#154861 - $15.00 USD Received 16 Sep 2011; revised 21 Oct 2011; accepted 26 Oct 2011; published 5 Dec 2011
(C) 2011 OSA

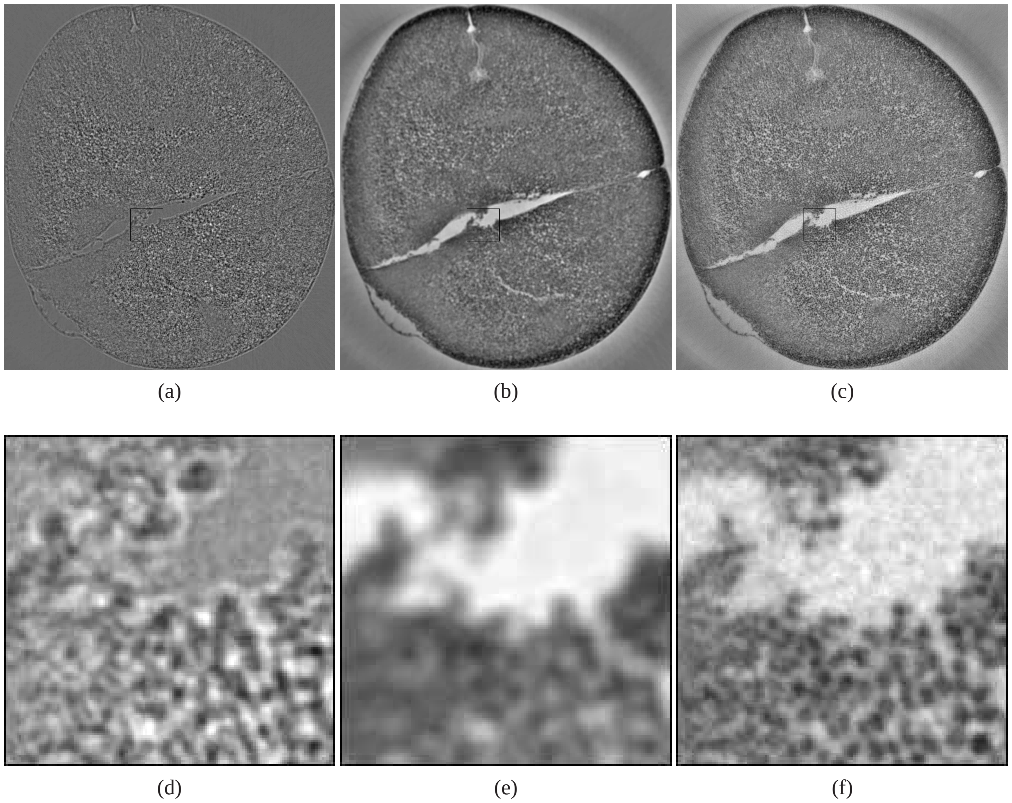

Fig. 6. Same object and experimental conditions as in Fig. 5. Shown is a 2-D slice of a tomographic reconstruction based on (a) intensity contrast, and on the phase retrieved according to (b) linearized TIE and (c) projected CTF with $\varepsilon = 0.01$. The images in the second row depict the quadratic regions of interest (ROIs) selected from the images in the first row. The width of the ROIs is 150 pixel, or 112 μm. In all images large-scale variations (mainly arising from small absorptive effects) were subtracted for better visibility.

contrast $\overline{\mathscr{F} g_z}(|\vec{\xi}|)$ which emerges at distance z under Fresnel propagation from a pure-phase induced exit-plane test map of realistic complexity. On one hand, an investigation was performed of the response of the position of the first minimum $|\vec{\xi}|_{min,1}$ of $\overline{\mathscr{F} g_z}(|\vec{\xi}|)$ to upscaling of the test map (scale factor S). For $S = 1$ phase variations were prepared to lie within the Fresnel scaling regime (symmetry under moderate upscaling, linearity). For a large range $1 \le S \le S_c$ the value of $|\vec{\xi}|_{min,1}$ is observed to be indifferent to upscaling: It stays at the first CTF "vacuum" $|\vec{\xi}|_1$. At $S_c = 356$, which corresponds to a maximal phase variation of about 3.6, *critical behavior* sets in which resembles a second-order like phase transition of critical exponent $\nu = 0.15 \pm 0.1$. (At $S_c = 356$ explicit breaking is supplemented by a *dynamical* breakdown of scaling symmetry, and $|\vec{\xi}|_{min,1} - |\vec{\xi}|_1$ is the associated pseudo-order parameter.) We have not in detail investigated other minima of $\overline{\mathscr{F} g_z}(|\vec{\xi}|)$, but, qualitatively, we see similar behavior. Therefore, cutting out thin rings around $|\vec{\xi}|_n$ ($n = 1, 2, 3, ...$) from the Fourier transform of the intensity contrast, as is done in projected CTF to enable regular phase retrieval at large values of S, works all the way up to S_c. On the other hand, we have shown that under upscaling the growth of the first maximum of $\overline{\mathscr{F} g_z}(|\vec{\xi}|)$ outraces the growth of the first minimum for $1 \le S \le S_c$. This can be

#154861 - $15.00 USD Received 16 Sep 2011; revised 21 Oct 2011; accepted 26 Oct 2011; published 5 Dec 2011
(C) 2011 OSA

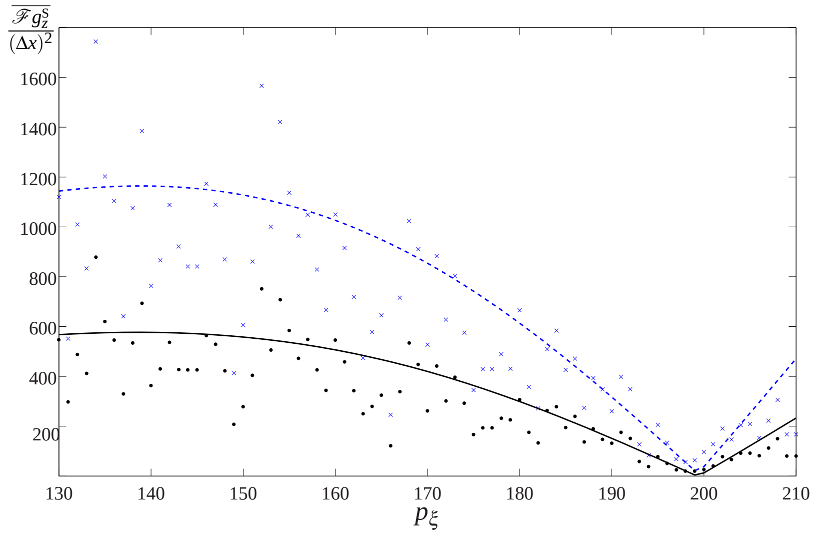

Fig. 7. Plots of function $\overline{\mathscr{F} g_z^S}(|\vec{\xi}|)$ in dependence of p_ξ. The black solid line is a fit (same fit function as in Fig. 1) to the data associated with Fig. 6(a),(d) ($S = 1$, data are black dots), and the dashed blue line is a fit to $\overline{\mathscr{F} g_z^S}(|\vec{\xi}|)$, obtained by an $S = 2$ (data are blue crosses) upscaling of retrieved phase using projected CTF, and a subsequent Fresnel forward propagation.

understood by the fact that the growth of maxima is generated linearly in S and locally in the Fourier transformed phase map $\mathscr{F}\phi_{z=0}$ while the growth of minima, albeit subject to higher powers in S, is due to successive autoconvolutions of $\mathscr{F}\phi_{z=0}$ which yield small coefficients generically. As a consequence, the omission of thin rings around $|\vec{\xi}|_n$ ($n = 1, 2, 3, \ldots$) from the Fourier transform of the intensity contrast keeps information loss at a low level. Therefore, it seems that below S_c the use of projected CTF for the retrieval of moderately strong phases is justified. We have applied projected CTF to the phase retrieval from single-distance intensity induced by an early-stage Xenopus embryo under coherent X-ray illumination. Moreover, we have shown self-consistency of projected CTF in this case by a moderate upscaling of the retrieved phase and subsequent Fresnel forward propagation, and we have performed a tomographic reconstruction of the biological sample.

Notice that in philosophy projected CTF is similar to Zernike phase contrast where a bias on the spectrum of the wave field is introduced at locations in Fourier space with no relevant information content [15, 16]. In Zernike phase-contrast microscopy this gives rise to useful intensity contrast. As we have shown in the present work, to retrieve phase in a local way in Fourier space from a single-distance intensity-contrast map, projected CTF may introduce a bias on the spectrum of the latter at fixed locations because the associated information loss is minimal.

Since projected CTF is single-distance and applicable to a wide range of relative phase variations it should be useful for real-time tomographic in vivo or in vitro phase-contrast imaging of compact developmental stages of optically opaque biological model systems such as Xenopus embryos [17].

Acknowledgments

We acknowledge the European Synchrotron Radiation Facility for provision of synchrotron radiation facilities, and we would like to thank Lukas Helfen for assistance in using beamline

ID19. We are grateful to L. Waller and H. Suhonen for useful conversations and to V. Altapova and D. Hänschke for the measurement of the Xenopus data. Finally, we would like to thank an anonymous Referee for constructive suggestions, leading, among other changes, to the implementation of Eqs. (4, 5) and Figs. 2, 7. We believe that theses suggestions have improved the paper substantially.

#154861 - $15.00 USD Received 16 Sep 2011; revised 21 Oct 2011; accepted 26 Oct 2011; published 5 Dec 2011
(C) 2011 OSA